PAPER

Reduction of EUV resist damage by neutral beam etching

To cite this article: Gyo Wun Kim *et al* 2022 *Nanotechnology* **33** 095301

IOP Publishing Nanotechnology
Nanotechnology 33 (2022) 095301 (8pp) https://doi.org/10.1088/1361-6528/ac3bee

Reduction of EUV resist damage by neutral beam etching

Gyo Wun Kim[1,3], Won Jun Chang[1,3], Ji Eun Kang[1], Hee Ju Kim[1] and Geun Young Yeom[1,2,*]

[1] School of Advanced Materials Science and Engineering, Sungkyunkwan University, Suwon, 440-746, Republic of Korea
[2] SKKU Advanced Institute of Nano Technology (SAINT), Sungkyunkwan University, Suwon, 440-746, Republic of Korea

E-mail: gyyeom@skku.edu

Received 10 August 2021, revised 8 November 2021
Accepted for publication 22 November 2021
Published 9 December 2021

Abstract

Even though EUV lithography has the advantage of implenting a finer pattern compared to ArF immersion lithography due to the use of 13.5 nm instead of 193 nm as the wavelength of the light source, due to the low energy of EUV light source, EUV resist has a thinner thickness than conventional ArF resist. EUV resist having such a thin thickness is more vulnerable to radiation damage received during the etching because of its low etch resistance and also tends to have a problem of low etch selectivity. In this study, the radiation damage to EUV resist during etching of hardmask materials such as Si_3N_4, SiO_2, etc using CF_4 gas was compared between neutral beam etching (NBE) and ion beam etching (IBE). When NBE was used, after the etching of 20 nm thick EUV resist, the line edge roughness increase and the critical dimension change of EUV resist were reduced by $\sim 1/3$ and $\sim 1/2$, respectively, compared to those by IBE. Also, at that EUV etch depth, the root mean square surface roughness value of EUV resist etched by NBE was $\sim 2/3$ compared to that by IBE on the average. It was also confirmed that the etching selectivity between SiO_2, Si_3N_4, etc and EUV resist was higher for NBE compared to IBE. The less damage to the EUV resist and the higher etch selectivity of materials such as Si_3N_4 and SiO_2 over EUV resist for NBE compared to IBE are believed to be related to the no potential energy released by the neutralization of the ions during the etching by NBE.

Supplementary material for this article is available online

Keywords: extreme ultraviolet (EUV) lithography, line edge roughness (LER), critical dimension (CD), damage, neutral beam etching (NBE), ion beam etching (IBE)

(Some figures may appear in colour only in the online journal)

1. Introduction

As the semiconductor device size becomes smaller, the importance of the lithography, a technique forming semiconductor circuit patterns, is increasing further [1–4]. In the past, the size of the pattern was gradually reduced through multi-patterning using the ArF immersion lithography technology, but it reached the limit of the continuously decreasing pattern size [5–8]. Recently, extreme ultra violet (EUV) lithography technology which uses a light source having the wavelength of 13.5 nm instead of the ArF light source having the wavelength of 193 nm has been introduced to reduce the size of patterns in the field of logic and memory semiconductors [9–12]. However, the current EUV lithography shows some problems in expanding to various patterning applications. One of the biggest problems is the thin thickness of the EUV resist. It is known that the maximum thickness that a EUV resist is ~50 nm due to the low energy of EUV light source which leads to a low sensitivity to resist.

[3] Gyo Wun Kim and Won Jun Chang equally contributed to the work.
[*] Author to whom any correspondence should be addressed.

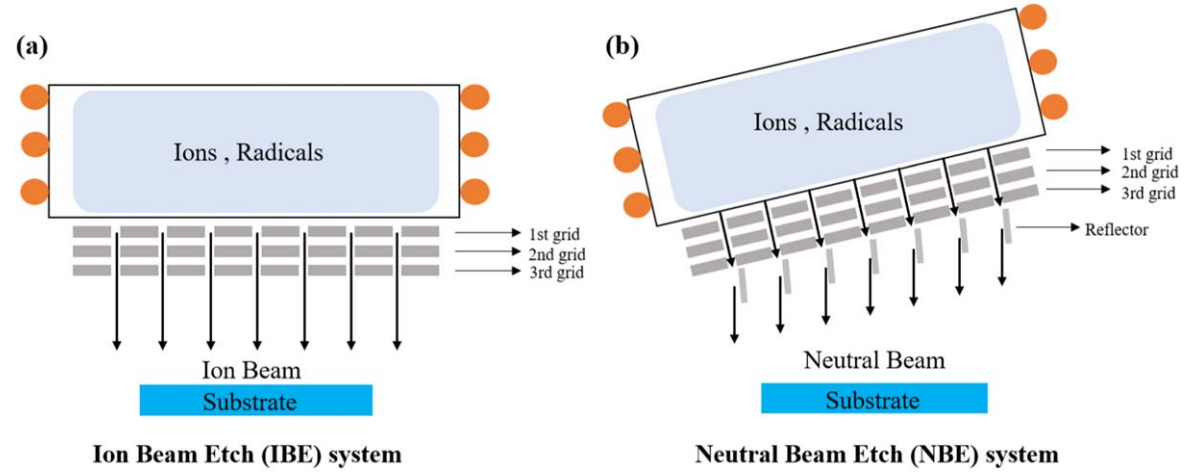

Figure 1. Schematic diagrams of (a) an IBE system and (b) a NBE system used in the experiment.

In addition to the low etch selectivity, such a thin resist is very vulnerable to damage received during the reactive ion etching (RIE) due to its low etch resistance [13–16].

Recently, studies are being conducted to reduce the damage to the EUV resist during the etching, and one of the most active studies is the addition of a metal in the EUV resist. The advantage of metal-containing resists compared to conventional chemically amplified resists is known to be the less damage during the etching by showing an improved line edge roughness (LER) and a higher etch resistance which can increase the etch selectivity over the hardmask materials such as SiO_2, Si_3N_4, Si, SiON, etc [17–22]. Despite these advantages, it has not been commercialized so far due to the difficulty in stripping the remaining metal containing resist after the etching. As an another technique, a cyclic etching method containing a polymer deposition and the preferential removal of the polymer layer on the SiON hardmask layer during the etch cycle has been also investigated to improve the etch selectivity and damage to the EUV resist during the etching [21, 23].

Previously, in order to minimize the electrical and physical damage to the semiconductor devices during the RIE, researches on neutral beam etching (NBE) have been actively conducted and the results showed the significant decrease in the charge related damage to the materials [24–26]. In addition, when a Si masked by a block co-polymer material such as polystyrene was etched using both a neutral beam and an ion beam, not only the improvement of etch damage to the block co-polymer but also a higher etch selectivity over Si was observed using a neutral beam [27].

In this study, the radiation damage to an EUV resist during the etching of hardmask materials such as Si_3N_4 and SiO_2 using a CF_4 neutral beam has been investigated and the results were compared with those etched by a CF_4 ion beam. The results showed, for the etching of the same EUV resist thickness, less LER, less critical dimension (CD) loss, and higher etch selectivity to the hardmask materials such as SiO_2 and Si_3N_4 were obtained for the CF_4 NBE compared to the CF_4 ion beam etching (IBE). To understand the differences in the etch mechanism, the differences in EUV resist etching between a neutral beam and an ion beam using non-reactive ions such as He and Ar were also studied.

2. Experiment

Figure 1 shows an IBE system and a NBE system used to compare the etch damage on EUV resist such as changes in LER and CD, and root mean square (RMS) surface roughness. The IBE system was composed of an inductively coupled plasma (ICP) type source and a 3-grid system made of graphite and, a positive voltage (+30 to +50 V) was applied to the 1st grid (acceleration grid) located close to the ICP source to control the energy of the ions and a negative voltage in the range of –30 to −100 V was applied to the 2nd grid to control the flux of the ions and to optimize the beam while the 3rd grid located near the sample was grounded. For the NBE system, the ICP source of the IBE system was tilted ∼10° and parallel reflector plates tilted ∼5° were attached below the 3rd grid to form a 5 degree-ion reflector for the neutralization of the ion beam extracted from the ion beam source.

As the samples, blank 50 nm thick negative-tone EUV resist coated on silicon wafer (SK siltron; p-type, ⟨100⟩, boron-doped, 10 ohm cm silicon) was used. SiO_2 and Si_3N_4 deposited on the same silicon wafers by low pressure chemical vapor deposition (∼200 nm in thickness using a furnace made by Centrotherm; Si_3N_4 deposition at 750 °C using dichlorosilane and NH_3. SiO_2 deposition at 700 °C using tetraorthosilicate) were used to investigate the etch rates and etch selectivities and to measure the etch surface roughness of EUV resist before and after the etching. Also, 50 nm thick negative-tone EUV resist patterned on a 50 nm thick BARC layer (bottom anti-reflective coating layer coated on silicon wafer) using a KrF lithography was used to measure the changes in LER (ΔLER) and the changes in CD (ΔCD) after the etching. For the etching, 1000 W of 13.56 MHz rf power was applied to the ICP source and 3 mTorr of CF_4 gas was used to etch blank EUV resist, SiO_2, and Si_3N_4, and line pattern of EUV resist. Also, 3 mTorr He and Ar gases were

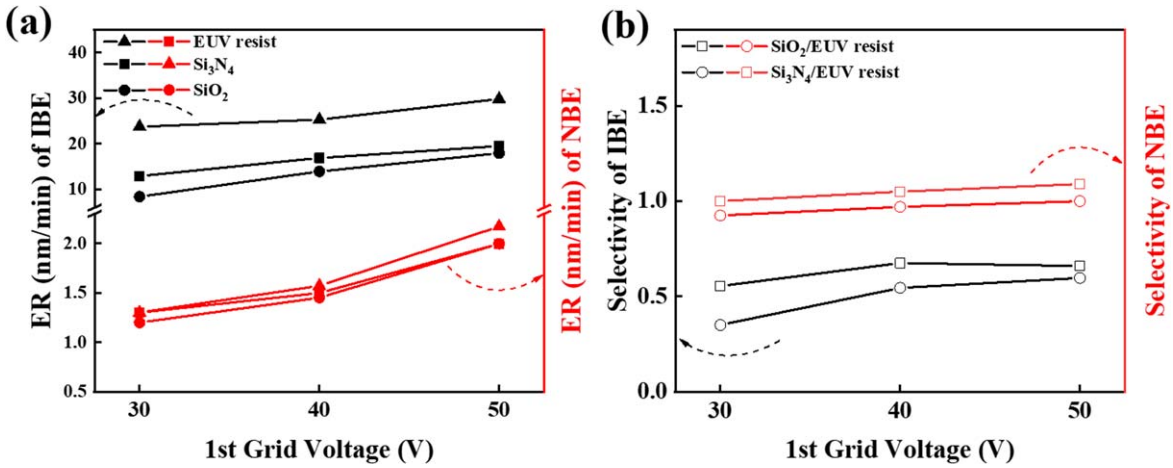

Figure 2. (a) Etch rates and (b) etch selectivities of EUV resist, SiO_2, and Si_3N_4 for IBE and NBE measured as a function of the 1st grid voltage using 3 mTorr CF_4 gas and 1000 W of ICP power. The etch depths of SiO_2 and Si_3N_4 etch depth were measured by using a spectroscopic ellipsometer.

also used to etch blank and patterned EUV resist to understand the etch mechanism.

The changes in etch characteristics of line patterned EUV resist such as LER and CD after the etching were observed by using a field emission scanning electron microscope (SEM, Hitachi S-4700), and the LER was measured by the Line and Contact Roughness Meter which is a Matlab based software (Lacerm). The etch depths of SiO_2 and Si_3N_4 were measured by using a spectroscopic ellipsometer (Nano-view SEMG-1000). The chemical binding states of the EUV resist before and after the etching with the CF_4 plasma were observed by x-ray photoelectron spectroscopy (XPS, Thermo VG, Multi-Lab 2000) and the surface roughness of blank EUV resist on the silicon wafer before and after etching was observed by using an atomic force microscope (AFM, NX-10).

3. Results and discussion

EUV resist coated on silicon wafer, SiO_2, and Si_3N_4 were etched using IBE and NBE and figures 2(a) and (b) show their etch rates and etch selectivites, respectively, measured as a function of 1st grid voltage. As process conditions, 3 mTorr of CF_4 gas was used with 1000 W of ICP power and the 1st grid was varied from +30 to +50 V. The etch rates of EUV resist, SiO_2, and Si_3N_4 were increased with the increase of 1st grid voltage due to the increased beam energy for both NBE and IBE. However, the NBE showed smaller etch rates than IBE for all samples at the same 1st grid voltage possibly due to the low reactivity of the neutral beam instead of the ion beam. The scattering of the ions from the parallel reflector during neutralization of the ion beam might be also related to the lower etch rates for NBE. Even though the etch rates are lower for NBE than IBE, as shown in figure 2(b), the etch selectivities of SiO_2/EUV resist and Si_3N_4/EUV resist were generally higher for NBE (SiO_2/EUV resist: 0.9–1.0 and Si_3N_4/EUV resist: 1.0–1.1) than IBE (SiO_2/EUV resist: 0.3–0.6 and Si_3N_4/EUV resist: 0.55–0.66). The etch selectivity of Si_3N_4 over EUV resist was a little higher than SiO_2 over Si_3N_4 due to the higher etch rate of Si_3N_4 by fluorine in the CF_4 gas.

EUV resist patterned on silicon wafer was also etched using the same etch conditions in figure 2 and the amount of change in CD (ΔCD) and LER (ΔLER) of EUV resist after the etching was measured for different 1st grid voltages (that is, different ion energies), and the results are shown in figures 3(a) and (b). For the different 1st grid voltages, the etch time was varied to etch 20 nm EUV resist (from 50 nm thick EUV resist) and 20 nm SiO_2 (from ~200 nm thick SiO_2) for figures 3(a) and (b), respectively. As shown in figures 3(a) and (b), there were no noticeable changes in ΔCD and ΔLER for patterned EUV resist when the EUV resist was exposed to the beam for the etch time required for etching of 20 nm EUV resist or 20 nm SiO_2 at the different 1st grid voltages for both NBE and IBE. However, there were significant differences in ΔCD and ΔLER of EUV resist between NBE and IBE. The ΔCD was 6.5–7.3 nm and the ΔLER was 1–1.2 nm for NBE while, for IBE, the ΔCD was 15.8 nm and the ΔLER was 3–3.5 nm. (Similar trends were observed for ΔCD and ΔLER of EUV resist after Si_3N_4 was 20 nm etched as shown in supplementary figure S1 available online at stacks.iop.org/NANO/33/095301/mmedia.) Therefore, it was found that, during the etching of same thickness of EUV resist or SiO_2, patterned EUV resist was more significantly damaged for IBE than NBE.

Figure 4 shows the actual SEM images of EUV resist pattern before and after the exposure for the time required to etch 20 nm Si_3N_4 (a), (d), SiO_2 (b), (e), and EUV resist (c), (f) using IBE and NBE with +50 V of the 1st grid voltage. As shown in the SEM images, the EUV resist widths were thinner after IBE than NBE and the ΔLER of etched EUV resist was also higher after IBE than NBE. (The SEM images of patterned EUV resist before and after the exposure for the time required to etch 20 nm thickness of SiO_2, Si_3N_4, and EUV resist by IBE and NBE with +30 V and +40 V are shown in supplementary figures S2 and S3, respectively.)

The changes in the RMS surface roughness of EUV resist after the exposure for the time required to etch 20 nm EUV resist at different 1st grid voltage using IBE and NBE were

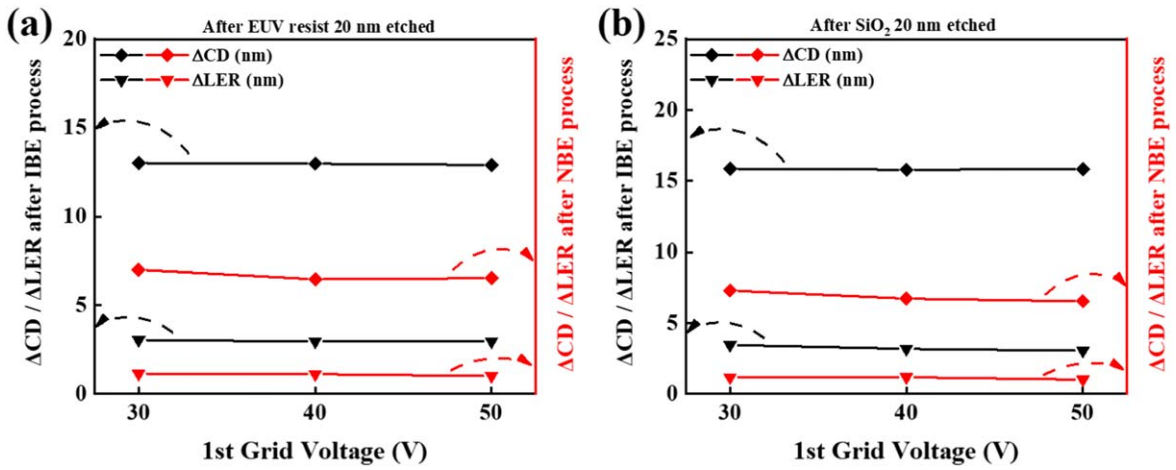

Figure 3. The amount of change in CD (ΔCD) and LER (ΔLER) of EUV resist after the etching using IBE and NBE for different 1st grid voltages for the etching (a) 20 nm of EUV resist and (b) 20 nm of SiO_2.

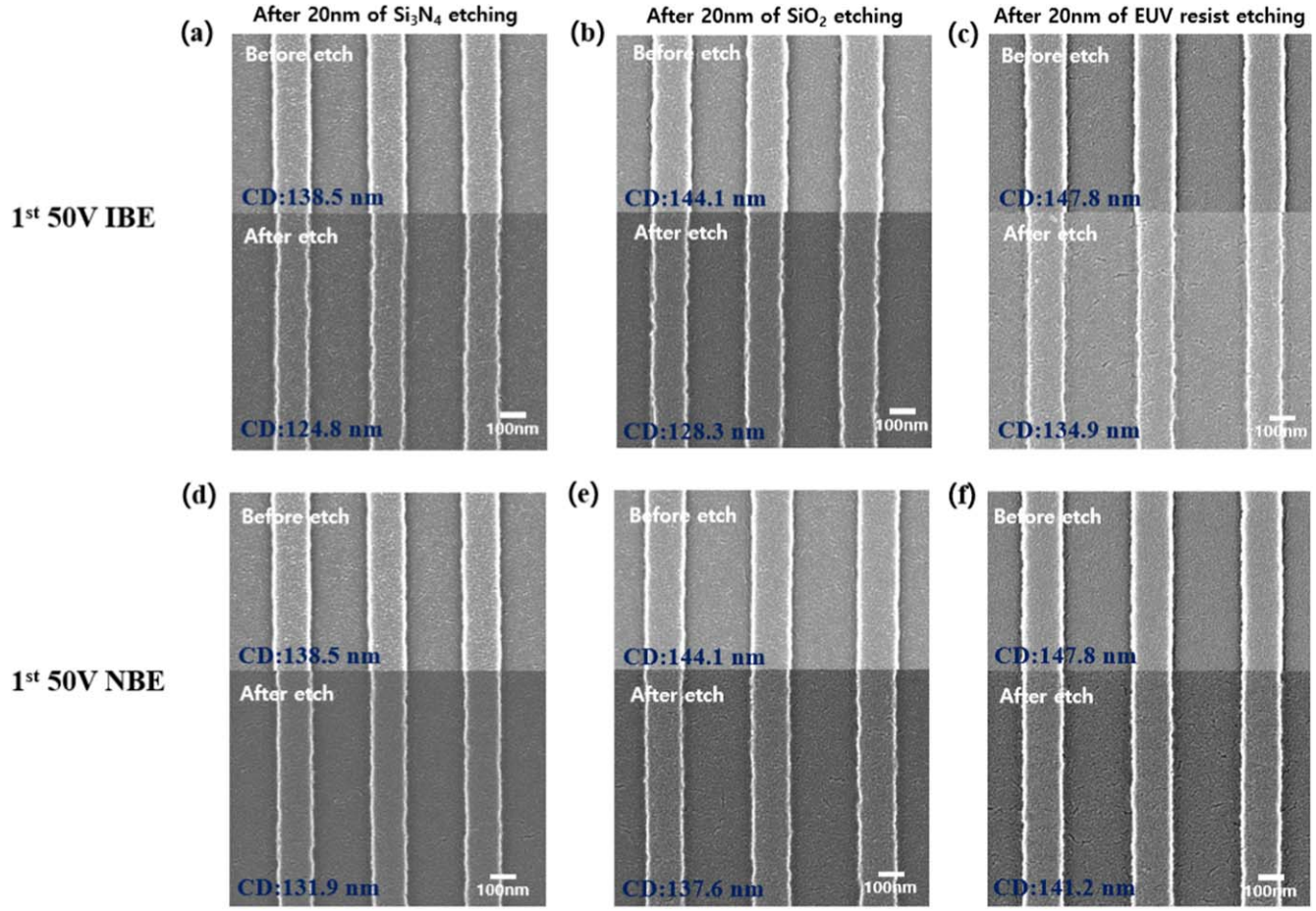

Figure 4. SEM images of EUV resist before and after the etching 20 nm of Si_3N_4 (a), (d), SiO_2 (b), (e), and EUV resist (c), (f) using IBE and NBE with 50 V of the 1st grid voltage.

observed using AFM and the surface roughness images and their RMS surface roughness values are shown in figure 5. The etch conditions are the same as those in figure 3(a). For IBE, the RMS surface roughness values were 3.12 nm at +30 V, 2.81 nm at +40 V, and 2.72 nm at +50 V, whereas, 1.83 nm at +30 V, 1.80 nm at +40 V, and 1.63 nm at +50 V for NBE. Therefore, slight decrease but no significant change in the surface roughness was observed with the increase of beam energy. However, similar to the ΔCD and ΔLER in figure 4, significant differences in RMS surface roughness values were observed between IBE and NBE confirming the smaller EUV resist damage by NBE than IBE.

XPS analysis was performed on the surfaces of EUV resist after 20 nm etching using CF_4 gas by IBE and NBE

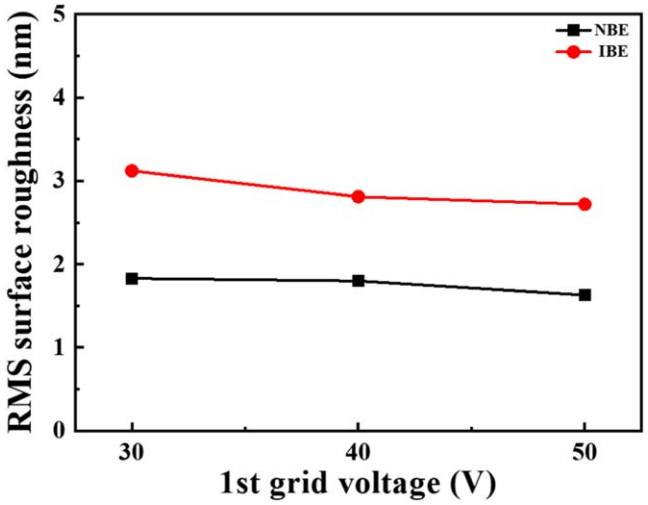

Figure 5. The RMS surface roughness values and the surface roughness images for different the 1st grid voltage for the etching 20 nm of EUV resist with CF_4 gas by IBE and NBE with the condition in figure 3(a). The initial thickness of EUV resist was 50 nm.

with +50 V of 1st grid voltage to investigate the differences in etching behavior between IBE and NBE. Figure 6(a) shows the atomic percentages of carbon, fluorine, and oxygen included in EUV resist before and after etching by IBE and NBE. In fact, in addition to carbon, fluorine, and oxygen, small traces of metal components were detected which are included in EUV resist for chemical amplification of the resist. As shown in figure 6(a), for the reference, small fluorine percentage of 3.6% originated from the original resist was observed and, after the IBE and NBE, due to the F radicals from the CF_4 plasma, F atomic percentage was increased to 33.9% for IBE and 38.7% for NBE, therefore, more fluorine percentage was observed on etched EUV resist surface for NBE compared to IBE. Figures 6(b)–(d) show the narrow scan data of C 1s for the EUV resist of the reference, after the IBE, and after the NBE, respectively. Compared to the reference, on the EUV resist surface etched with a CF_4 plasma, the carbon binding peaks related to C–F_x ($x = 1$, 2, and 3 at 289.5 eV, 291.6 eV, and 293.7 eV, respectively), C–O (286.3 eV), and CO–CF_x (287.7 eV) could be deconvoluted in addition to the main C–C peak at 284.8 eV [28]. The C 1s data shown in figures 6(c) and (d) show higher C–F_x related peaks for the EUV resist etched by NBE compared to that etched by IBE. XPS depth profiling was also performed on the EUV resist surface etched by NBE and IBE but, after the 1st depth profiling cycle, the C–F_x related peaks were almost removed for both EUV resists etched by NBE and IBE, therefore, it is believed that the fluorinated carbon layer is formed only on the EUV resist thin surface during the etching (not shown). The higher C–F_x bonding peaks on the EUV resist etched by NBE compared to those by IBE are possibly related to the longer exposure time of EUV resist to CF_x radicals for the etching of 20 nm depth of EUV resist, therefore, more adsorption of CF_x on the etched EUV surface for NBE. (The surfaces of EUV resist etched by NBE and IBE using an Ar plasma instead of a CF_4 plasma were also investigated by XPS and the results are shown in supplementary table S1 for the EUV surface composition and figure S4 for C 1s narrow scan data before and after etching by NBE and IBE. As shown in table S1, the composition of EUV resist was changed after the 20 nm etching by both NBE and IBE, but no significant compositional differences between the EUV surfaces etched by NBE and IBE could be observed. Also, figure S4 shows the narrow scan data of C 1s peak on the EUV surfaces etched by NBE and IBE and no significant differences between the IBE and NBE were also observed. There are no radicals for the Ar plasma while CF_x radicals exist for a CF_4 plasma. For the etching using a CF_4 plasma, the etch time for NBE is much longer than that for IBE and, the EUV surface will be exposed to CF_x radicals more time for NBE while there are no differences in radical amount and species between NBE and IBE except for the beam itself.) XPS depth profiling was also performed on the EUV resist surface etched by NBE and IBE but, after the 1st depth profiling cycle, the C–F_x related peaks were almost removed for both EUV resists etched by NBE and IBE, therefore, it is believed that the fluorinated carbon layer is formed only on the EUV resist thin surface during the etching (not shown).

To understand the differences in the damage of EUV resist such as surface roughness and LER between IBE and NBE, inert gases such as He and Ar were used for the ICP ion beam instead of a reactive CF_4 gas, and the change in characteristics of EUV resist was investigated. Figures 7(a) and (b) show the ΔLER and RMS surface roughness of EUV resist after etching 10 nm from 50 nm thick EUV resist, respectively, using He and Ar with IBE at +50 V of 1st grid voltage and with NBE at +50 to +100 V of 1st grid voltage. As shown in figure 7(a), similar to CF_4 gas, at the same 1st grid voltage of +50 V, the IBE showed higher ΔLER of 3.84 nm compared to 2.03 nm for NBE with Ar gas. In the case of He, the IBE showed ΔLER of 2.51 nm while NBE showed 1.1 nm, therefore, the ΔLER was a little lower for He compared to Ar but IBE also showed higher ΔLER compared to NBE. As shown in figure 7(b), the RMS surface roughness values were also lower for the NBE by showing 1.15 nm (Ar) and 0.84 nm (He) compared to 2.6 nm (Ar) and 1.14 nm (He) for IBE. In the case of NBE, the ΔLER and RMS surface roughness of EUV resist with increasing 1st grid voltage from +50 to +100 V were also measured after the etching of 10 nm from 50 nm thick EUV resist with Ar and He. As shown in figures 7(a) and (b), the increase of beam energy up to +100 V did not change the ΔLER and RMS surface roughness of EUV resist significantly. (The actual SEM images of ΔLER and AFM images of surface roughness for figure 7 can be found in supplementary figures S5–S7.)

Figure 8 shows possible differences in the damage mechanism of EUV resist between IBE and NBE (yellow color arrow: momentum transfer, red color arrow: potential energy released by ion neutralization, blue color: incident and reflected ions/neutrals, green color: removed atoms/molecules). During the etching of EUV resist by NBE and IBE, by the kinetic energy of the incident ions/neutrals, momentum is transferred to EUV resist for the etching and, during the

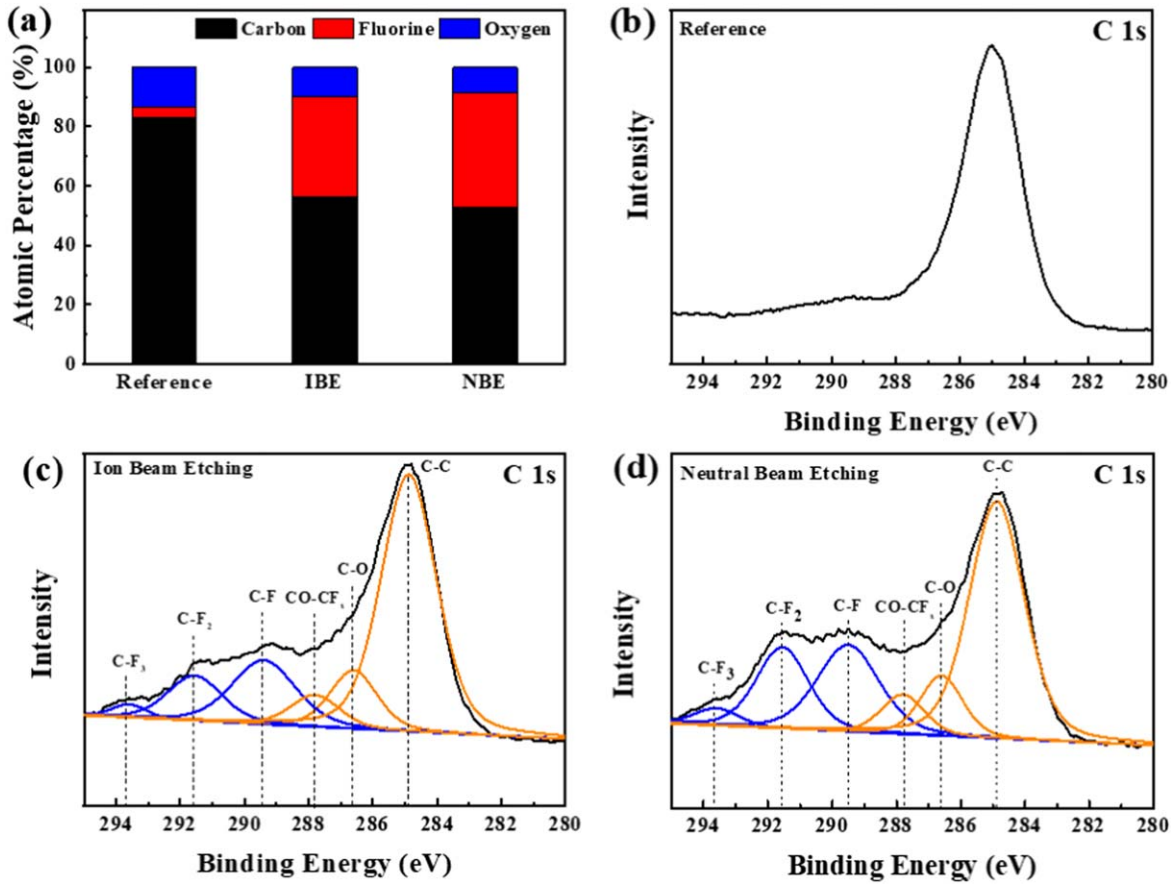

Figure 6. (a) Atomic percentages of EUV resist surface before and after etching 20 nm from 50 nm thick EUV resist using IBE and NBE at +50 V of 1st grid voltage with a CF_4 gas. XPS narrow data of C 1s of (b) before etching EUV resist (reference), (c) after etching 20 nm of EUV resist using IBE, and (d) after etching 20 nm of EUV resist using NBE.

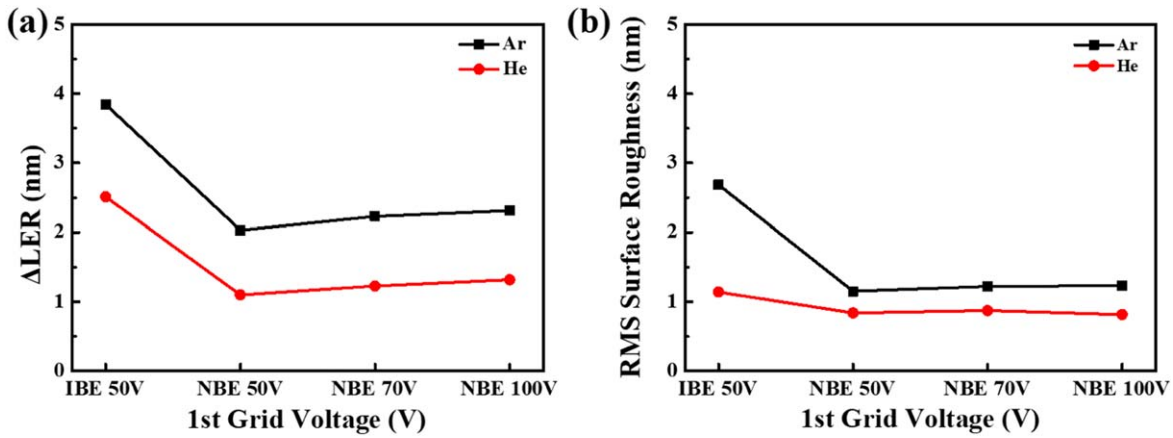

Figure 7. (a) ΔLER and (b) RMS surface roughness value of EUV resist after etching 10 nm from 50 nm thick resist using He and Ar with IBE at +50 V of 1st grid voltage and with NBE at +50 to 100 V of 1st grid voltage.

momentum transfer, the surface of EUV resist can be damaged physically. In addition, if there is a potential energy release by the neutralization of the ions on the EUV resist surface, it can cut the EUV resist bonding and can also damage the EUV resist surface in addition to the release of energy for the vaporization of the etch compounds formed on the surface. The higher EUV resist surface damage observed in the etching with inert gases for IBE compared to NBE shown in figure 7 in addition to the higher damage with a reactive CF_4 gas for IBE shown in figures 2–5 appears to be related to the release of ionization potential energy during the neutralization of the ions. In fact, the ionization potential of He is ∼24.5 eV while that of Ar is ∼15.8 eV [29, 30], therefore, He will release a higher potential energy during the neutralization but Ar showed higher EUV resist surface damage possibly due to the additional damage by the higher

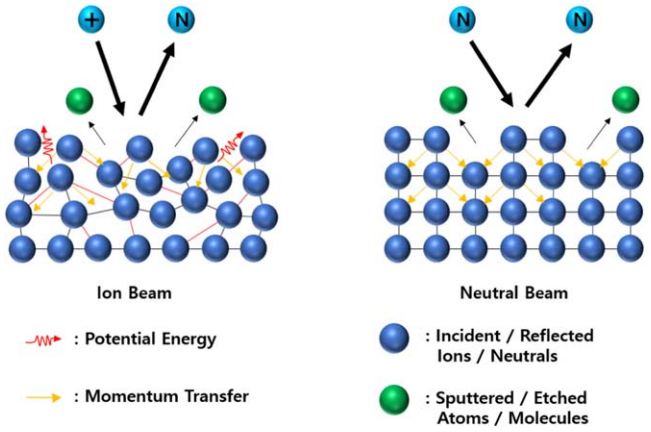

Figure 8. Possible differences in damage mechanism of EUV resist between IBE and NBE.

momentum transfer to the EUV resist. The higher etch selectivities observed for NBE compared to IBE might be also related to the lack of the energy release by neutralization on the materials surfaces during the etching for NBE. Therefore, by using NBE instead of IBE (or generally, RIE), not only the decrease of EUV resist surface damage but also increased etch selectivity of materials such as SiO_2 and Si_3N_4 over EUV resist could be obtained.

4. Conclusion

In this study, the radiation damage to EUV resist such as the increased RMS surface roughness and the changes in CD (ΔCD) and LER (ΔLER) during the etching of SiO_2 and Si_3N_4 using a CF_4 gas were compared between NBE and IBE. The etch selectivities of SiO_2 and Si_3N_4 over EUV resist were higher for NBE compared to IBE, and ΔCD and ΔLER were lower for NBE compared to IBE. In addition, when blank EUV resist was etched by IBE and NBE with a CF_4 gas, the RMS surface roughness value was lower for NBE compared to IBE confirming that NBE can reduce the damage to EUV resist compared to IBE. A neutral beam has only a kinetic energy which causes momentum transfer to the surface of EUV resist, but an ion beam has a kinetic energy and an ionization potential energy which can not only cause momentum transfer on the surface on EUV resist by kinetic energy, but also cause the bond breaking of EUV resist due to the release of ionization potential energy during the neutralization of the ions. Therefore, the lower damage to the EUV resist and the higher etch selectivity for NBE are believed to be related to the no ionization potential energy released on the materials surface by the neutralization of the ions during the etching by NBE.

Acknowledgments

This work was supported by Samsung Electronics Co., Ltd. (IO201211–08086–01) and by Nano Material Technology Development Program through the National Research Foundation of Korea (NRF) funded by the Ministry of Education, Science and Technology (2021M3H4A1A02055667). And thanks to Dongwoo Fine-Chem for providing EUV resist wafers.

Data availability statement

The data that support the findings of this study are available upon reasonable request from the authors.

ORCID iDs

Geun Young Yeom https://orcid.org/0000-0001-6603-2193

References

[1] Thompson L F, Willson C G and Bowden M J 1983 An introduction to lithography *Introduction to Microlithography* (Washington, DC: American Chemical Society)
[2] Pimpin A and Srituravanich W 2012 Reviews on micro- and nanolithography techniques and their applications *Eng. J.* **16** 37–55
[3] Pease R F and Chou S Y 2008 Lithography and other patterning techniques for future electronics *Proc. IEEE* **96** 248–70
[4] Stulen R H and Sweeney D W 1999 Extreme ultraviolet lithography *IEEE J. Quantum Electron.* **35** 694–9
[5] Bencher C, Chen Y, Dai H, Montgomery W and Huli L 2008 22 nm half-pitch patterning by CVD spacer self alignment double patterning (SADP) *Opt. Microlithogr.* **6924** 69244E
[6] Xu P *et al* 2011 Sidewall spacer quadruple patterning for 15 nm half-pitch *Opt. Microlithogr.* **7973** 79731Q
[7] Nakagawa H, Fujisawa T, Goto K, Kimura T, Kai T and Hishiro Y 2011 Ultra-thin-film EUV resists beyond 20 nm lithography *Adv. Resist Mater. Process. Technol.* **7972** 79721I
[8] Arnold W H, Dusa M and Flinders J 2007 Metrology challenges of double exposure and double patterning *Metrol. Insp. Process Control Microlithogr.* **6518** 651802
[9] Neisser M and Wurm S 2015 ITRS lithography roadmap: 2015 challenges *Adv. Opt. Technol.* **4** 235–40
[10] Eom T S, Kim H I, Kang C K, Ryu Y J, Hwang S H, Lee H H, Lim H Y, Park J S, Kwak N J and Park S 2013 Patterning challenges of EUV lithography for 1X-nm node DRAM and beyond *Extrem. Ultrav. Lithogr.* **8679** 86791J
[11] Ha D *et al* 2017 Highly manufacturable 7nm FinFET technology featuring EUV lithography for low power and high performance applications *Dig. Tech. Pap.—Symp. VLSI Technol.* pp T68–9
[12] Lio A 2016 EUV resists: What's next ? *Extrem. Ultrav. Lithogr.* **9776** 97760V EUV resists: What's next?
[13] Wood O R 2017 EUVL: Challenges to manufacturing insertion *J. Photopolym. Sci. Technol.* **30** 599–604
[14] Trikeriotis M, Krysak M, Chung Y S, Ouyang C, Cardineau B, Brainard R, Ober C K, Giannelis E P and Cho K 2012 A new inorganic EUV resist with high-etch resistance *Extrem. Ultrav. Lithogr.* **8322** 83220U
[15] Manouras T and Argitis P 2020 High sensitivity resists for EUV lithography: a review of material design strategies and performance results *Nanomaterials* **10** 1–24

[16] Luo C, Xu C, Lv L, Li H, Huang X and Liu W 2020 Review of recent advances in inorganic photoresists *RSC Adv.* **10** 8385–95
[17] De Simone D *et al* 2016 Demonstration of an N7 integrated fab process for metal oxide EUV photoresist *Extrem. Ultrav. Lithogr.* **9776** 97760B
[18] Li L, Liu X, Pal S, Wang S, Ober C K and Giannelis E P 2017 Extreme ultraviolet resist materials for sub-7 nm patterning *Chem. Soc. Rev.* **46** 4855–66
[19] Grenville A *et al* 2015 Integrated fab process for metal oxide EUV photoresist *Adv. Patterning Mater. Process.* **9425** 94250S
[20] Lewis S M *et al* 2019 Plasma-etched pattern transfer of sub-10 nm structures using a metal-organic resist and helium ion beam lithography *Nano Lett.* **19** 6043–8
[21] Mao M, Lazzarino F, De Schepper P, De Simone D, Piumi D, Luong V, Yamashita F, Kocsis M and Kumar K 2017 Patterning with metal-oxide EUV photoresist: patterning capability, resist smoothing, trimming, and selective stripping *Adv. Patterning Mater. Process.* **10146** 101460I
[22] De Simone D, Pollentier I and Vandenberghe G 2015 Metal-containing materials as turning point of EUV lithography *J. Photopolym. Sci. Technol.* **28** 507–14
[23] Park J H, Kim S G and Yeom G Y 2021 Session PS2 + EM plasma etch solutions for defect reduction in ultra-thin photoresist *AVS 67th Int. Symp. & Exhibition* pp 1–275
[24] Kang S H, Kim J K, Lee S H, Kim J W and Yeom G Y 2015 Low damage etching method of low-k material with a neutral beam for interlayer dielectric of semiconductor device *J. Vac. Sci. Technol.* A **33** 021309
[25] Samukawa S 2007 High-performance and damage-free neutral-beam etching processes using negative ions in pulse-time-modulated plasma *Appl. Surf. Sci.* **253** 6681–9
[26] Min K S *et al* 2013 Improvement of metal gate/high-k dielectric CMOSFETs characteristics by neutral beam etching of metal gate *Solid State Electron.* **86** 75–8
[27] Yun D, Park J, Kim H, Mun J, Kim S, Kim K and Yeom G 2016 Improvement of a block co-polymer (PS-b-PMMA)-masked silicon etch profile using a neutral beam *Nanotechnology* **27** 384002
[28] Coulon J F and Turban G 1991 An XPS study of photoresist surfaces in SF6O2 r.f. plasmas *Mater. Sci. Eng.* A **139** 385–93
[29] Hammond R H, Henis J M S, Greene E F and Ross J 1971 Kinetic energies of lonization products from collisions of Ar-Ar, He-He below 150 eV c.m. energy *J. Chem. Phys.* **55** 3585–8
[30] Müller A, Achenbach C and Salzborn E 1979 Dependence of the charge transfer between atoms and highly charged ions on the ionization potential of the atoms *Phys. Lett.* A **70** 410–2